Gas-phase silicon micromachining with xenon difluoride

Floy I. Chang, Richard Yeh, Gisela Lin, Patrick B. Chu, Eric Hoffman, Ezekiel J. J. Kruglick, and Kristofer S.J. Pister

Micro-Electro Mechanical Systems Laboratory
Department of Electrical Engineering
University of California at Los Angeles
405 Hilgard Avenue, Los Angeles, CA 90095-1594

Michael H. Hecht

Jet Propulsion Laboratory, California Institute of Technology
4800 Oak Grove Drive, Pasadena, CA 91109

ABSTRACT

Xenon difluoride (XeF_2) is a gas phase, room temperature, isotropic silicon etchant with extremely high selectivity to many materials commonly used in microelectromechanical systems (MEMS), including photoresist, aluminum, and silicon dioxide. Using a simple vacuum system, the effects of etch aperture and loading were explored for etches between 10 and 200μm. Etch rates as high as 40μm/minute were observed. Initial characterization of wafer surface temperature during the etch indicates tens of degrees of self-heating, which is known to cause substantial decrease in etch rate.

Keywords: XeF_2, gas-phase etching, bulk micromachining

1. INTRODUCTION

There are a variety of silicon etchants available today for bulk-micromachining ranging from conventional liquid-phase chemical etchants such as EDP, KOH, TMAH, and HNA[1,2] to high energy plasma etchants involving Cl and SF_6. These indispensable etchants offer the control and versatility to fabricate MEMS devices such as accelerometers, pressure sensors, microphones, microvalves, etc. However, there are some limitations associated with these etchants, including lack of a simple masking material such as photoresist, insufficient selectivity to aluminum and other common MEMS materials, and structure damage due to bubble formation and other etching and rinsing forces.

Xenon difluoride (XeF_2) is a dry, isotropic vapor-phase silicon etchant that offers some advantages over the traditional silicon etchants. At room temperature and atmospheric pressure, it is a white crystalline solid which sublimates at its vapor pressure (~3.8Torr at 25°C) to etch silicon. Some of the main advantages of using XeF_2 are its high selectivity to aluminum, photoresist, and silicon dioxide, its gaseous phase which minimizes adhesion or stiction problems, its isotropic etch property which allows large structures to be undercut quickly, and its fast etch rate of tens of microns per minute when etching areas on the order of a few square millimeters or less. However, like other etchants, XeF_2 has some disadvantages. XeF_2 has no known silicon etch stops, no crystal plane selectivity, and does not display the substantially lower P+ etch rate found in most silicon etchants.

In 1962, Neil Bartlett synthesized the first noble gas compound, $XePtF_6$ [3], and XeF_2 was discovered shortly thereafter[4]. The first paper documenting the etching of silicon with XeF_2 vapor was published in 1979 by Winters and Coburn[5], who investigated the variation of etch rate with pressure and described the selectivity of XeF_2 for different silicon compounds. Further investigations were conducted by Houle[6] and Flamm et al.[7] Although XeF_2 has been a known silicon etchant for the past sixteen years, only recently has it been used in the fabrication of MEMS structures. In 1994, Hoffman et al.[8] created 3-dimensional structures with piezoresistive sensors in a standard CMOS process using XeF_2 to bulk micromachine the chips. Several examples of XeF_2 etched structures can be found elsewhere in these proceedings [9,10,11]. This paper presents some of the properties of this interesting etchant.

0-8194-2007-7/95/$6.00

Downloaded From: http://proceedings.spiedigitallibrary.org/ on 10/23/2015 Terms of Use: http://spiedigitallibrary.org/ss/TermsOfUse.aspx

2. ETCHING MECHANISM

The primary reaction that takes place between XeF_2 and silicon is given below:

$$2XeF_2 + Si \rightarrow 2Xe + SiF_4 \quad (1)$$

This reaction consists of a sequence of steps: 1) non-dissociative adsorption of XeF_2 at the silicon surface; 2) dissociation of the absorbed gas, F_2; 3) reaction between the adsorbed atoms and the silicon surface to form an adsorbed product molecule, SiF_4 (ads); 4) desorption of the product molecule into the gas phase; and 5) the removal of non-reactive residue from the etched surface [12]. The primary reaction product, SiF_4, is volatile at room temperature, as is the etch residue, dissociated Xe. There is some disagreement in the literature as to the exact by-products of the XeF_2-Si reaction. However, most groups agree that SiF_4 is the dominant reaction product, with significant amounts of SiF_2 also formed during the reaction [13].

3. ETCHING SETUP AND METHODS

In the experiments described in sections four, five, and seven, 3-inch <100> phosphorous-doped n-type silicon wafers with a resistivity of 0.007-0.011Ω-cm were used. Note that these are heavily doped n-type substrates. The wafers ranged from 356μm to 406μm thick. Silicon etch windows were patterned with thermal oxide, photoresist†, or aluminum mask layers. Additional photoresist was painted on the silicon wafer edges and undersides to prevent etching in those areas. In the experiments described in section six, chips fabricated in Orbit Semiconductor's 2μm, double-polysilicon, p-well process were used. XeF_2 was obtained from commercial vendors[14,15,16] and all experiments were conducted at room temperature (~22°C) under standard laboratory illumination.

All samples were dehydrated in an oven at 120°C for at least 5 minutes. If samples are not dehydrated, a white cloudy film has been seen to form shortly after etching begins. This film has a dramatic effect on the etch rate, and may completely stop etching. This film may be a silicon fluoride polymer, similar in structure to PTFE, formed by a reaction between the XeF_2, silicon, and a surface water layer on the silicon[17]. The presence of moisture may also explain the slight etching of silicon dioxide which has been observed occasionally on samples which were not dehydrated. The mechanism of silicon dioxide etching is presumed to be the formation of HF by decomposition of XeF_2 in the presence of water.

3.1 Setup

A diagram of the etching setup is shown in Figure 1. The etching system consists of a glass etching chamber connected to a vacuum pump, pressure meter, electrical feed-throughs, nitrogen inlet, and stainless steel XeF_2 source bottle. Materials used in constructing the system include glass, stainless steel, aluminum, and o-rings*, though degradation of the o-rings over the course of a year has been observed. XeF_2 crystals are poured into the source bottle under a fume hood. Generally the bottle is filled with between one and ten grams of XeF_2. The sample is clamped to an aluminum mount during etching.

3.2 Pulse Etching

Two different etching methods were used for the experiments described in this study. The first method is "pulse etching," in which the sample to be etched is alternately exposed to XeF_2 vapor and vacuum. The steps are outlined as follows:

(1) The etch chamber is pumped down to vacuum (~20mTorr) then all valves are closed.
(2) The XeF_2 inlet valve is opened and the timing for a pulse duration begins.
(3) The XeF_2 inlet valve is closed when the chamber pressure reaches a desired value (i.e. 2500mTorr).
(4) The XeF_2 stays in the chamber until the desired pulse duration is reached.
(5) The chamber is pumped back down to vacuum, and the cycle repeats.

The time to reach target pressure is determined by the chamber volume and the sublimation rate of XeF_2. For our chamber, which is several liters in volume, a pressure of 2500mT is reached in approximately 20 seconds.

†. OCG 825 35S positive resist and Hoechst-Celanese AZ5214-E photoresist.
* Du Pont Viton® flouroelastomer o-ring.

Downloaded From: http://proceedings.spiedigitallibrary.org/ on 10/23/2015 Terms of Use: http://spiedigitallibrary.org/ss/TermsOfUse.aspx

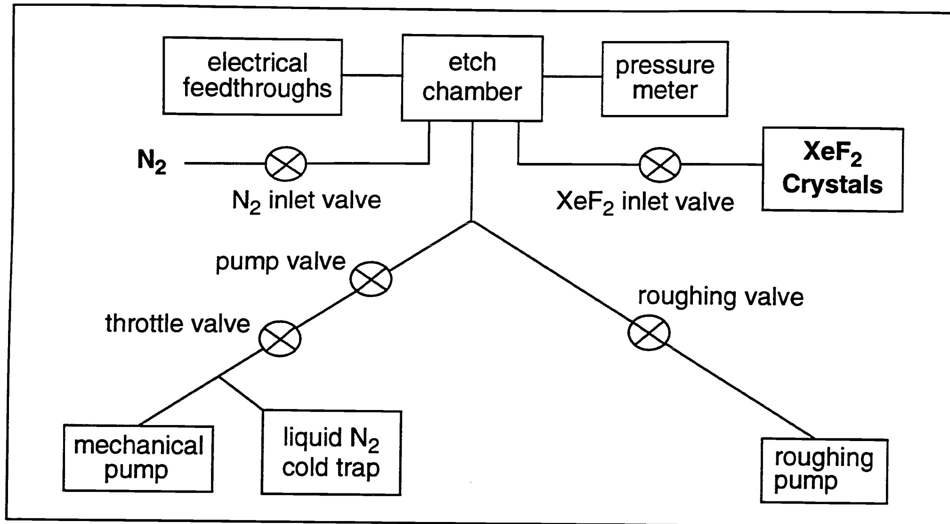

Fig. 1. Diagram of the XeF_2 etching system used in this study.

3.3 Constant Pressure Etching

The second method consists of etching at a constant pressure for a designated amount of time, which is easier and more convenient for longer etching times. This method is outlined below:

(1) The chamber is initially at vacuum (~20mTorr) with the pump and throttle valves open (roughing valve closed).
(2) The XeF_2 inlet valve is opened to begin etching.
(3) The pressure is immediately adjusted to the desired etch pressure (typically 2500mTorr) using the throttle valve.
(4) The XeF_2 inlet valve is closed when the desired etch time is reached.
(5) The chamber is pumped back down to vacuum.

It typically takes less than a minute to stabilize the pressure after the XeF_2 inlet valve is opened. One gram of XeF_2 lasts for roughly one hour under either of the etching conditions described above, although this has not been well characterized. In small quantities, the cost of one gram of XeF_2 is roughly $12[15].

4. SELECTIVITY AND ETCH RATES

XeF_2 has shown a selectivity of greater than 1000:1 to the following materials: silicon dioxide, OCG 825 and AZ 5214 photoresist, several polyimides, aluminum, copper, gold, titanium-nickel alloy, and acrylic. Figure 2 contains photographs taken using a scanning electron microscope (SEM). The photos on the left show aluminum, thermal silicon dioxide, and photoresist clamped-clamped beams which were patterned on silicon and released in XeF_2. Each etch was 10-12 minutes long at a constant pressure of 2500mTorr. The etch depth ranges from 40 to 50μm, while the lateral undercut ranges from 30 to 40μm. The aluminum beams are 1500Å thick, the oxide beams are 0.5μm thick, and the photoresist beams are 2μm thick. As shown, there was no apparent etching of the beam materials, demonstrating the high selectivity of XeF_2. The shape of the beams indicates that the aluminum and photoresist films are under tension, while the silicon dioxide is under compression, as expected. In addition to these tests, two aluminum samples, one exposed to XeF_2 and one not, were scanned using an AFM. The surface profiles indicate no apparent effect on aluminum by exposure to XeF_2.

The photos on the right in Figure 2 show clamped-free cantilever beams that were etched in XeF_2 for 10-12 minutes at a constant pressure of 2500 mTorr. The dimensions of these beams, the etch depth, and the amount of undercut are similar to those of the clamped-clamped beams. The bending of the aluminum beams can be attributed to either charging in the SEM or plastic deformation due to the air flow during SEM chamber pumpdown. The curling of the silicon dioxide beams is probably due to residual stress, and the curvature seen in the photoresist beams is most likely due to a combination of residual stress and

Downloaded From: http://proceedings.spiedigitallibrary.org/ on 10/23/2015 Terms of Use: http://spiedigitallibrary.org/ss/TermsOfUse.aspx

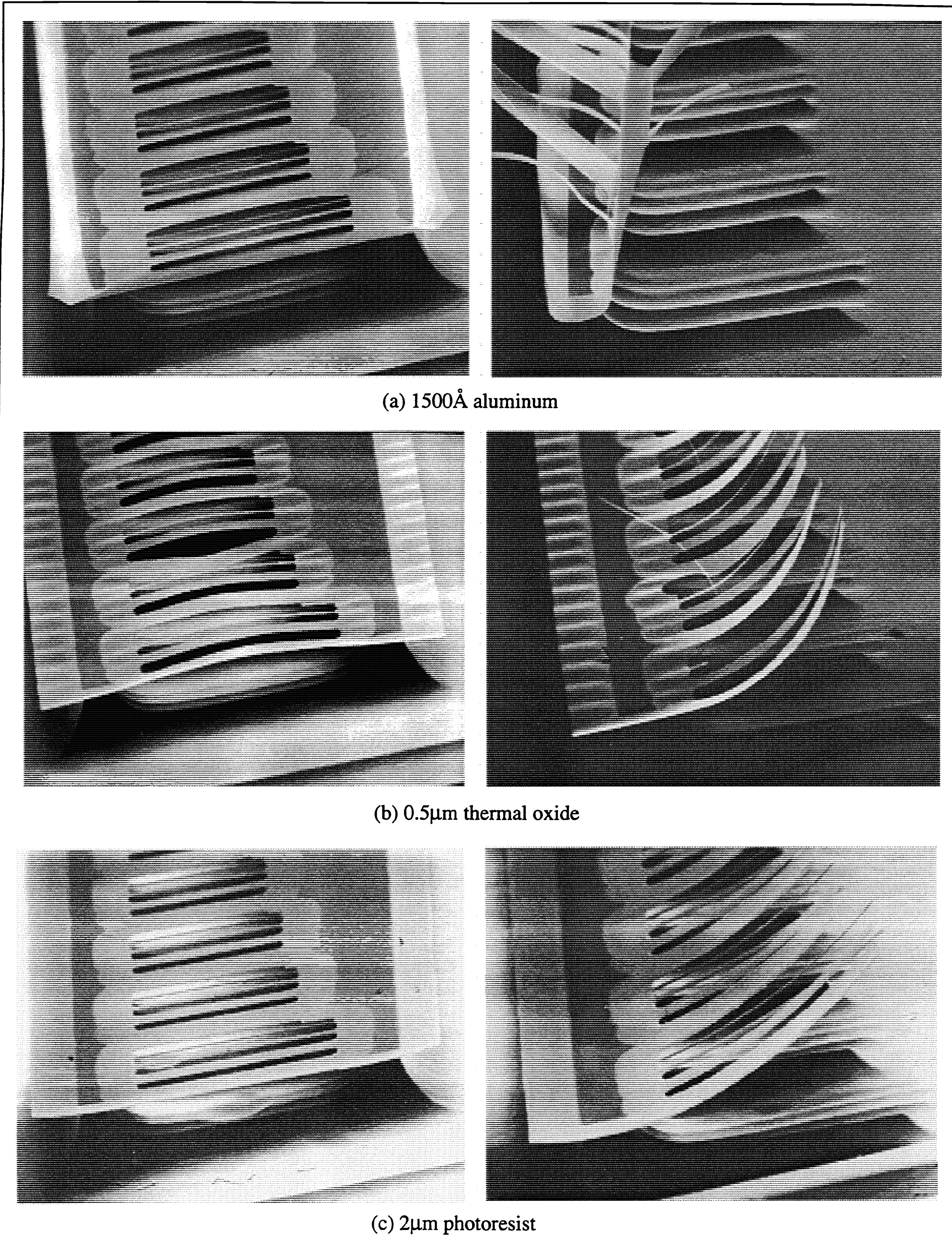

(a) 1500Å aluminum

(b) 0.5μm thermal oxide

(c) 2μm photoresist

Fig. 2. SEM photographs of clamped-clamped (left) and clamped-free (right) beams etched in XeF_2. Beam width varies from 2-50μm and the longest beams shown are 200μm long. The etch depth was ~50μm, and the beam material and thickness are listed below each pair of photographs.

Downloaded From: http://proceedings.spiedigitallibrary.org/ on 10/23/2015 Terms of Use: http://spiedigitallibrary.org/ss/TermsOfUse.aspx

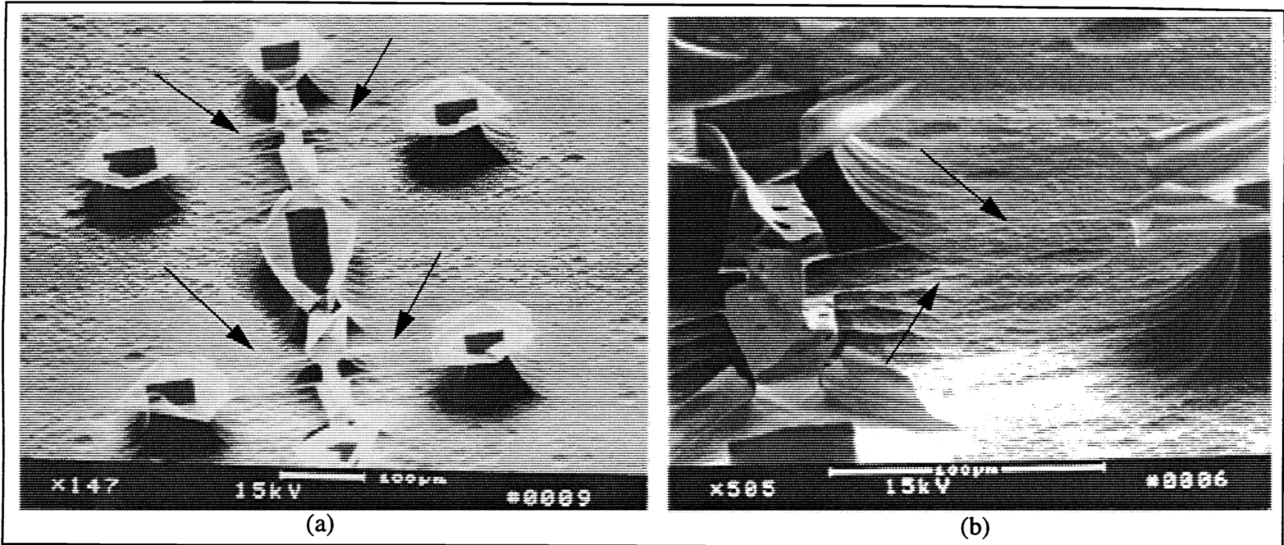

Fig. 3. SEM photographs of 2μm wide, 240μm long clamped-clamped beams made of 400Å thick thermal oxide. The silicon etch depth is roughly 50μm. (a) The beams are indicated by arrows. (b) Close-up of the beams in (a).

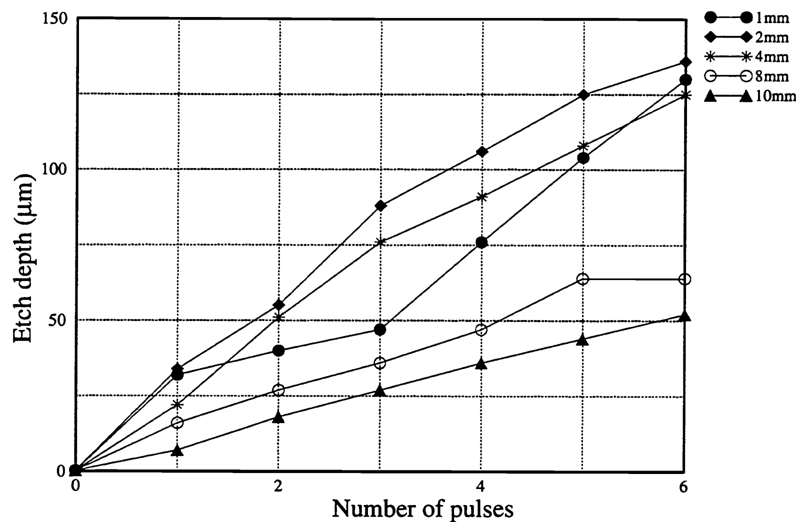

Fig. 4. Graph of etch depth vs. number of pulses for isolated square apertures of different sizes, illustrating the loading effect. Legend indicates side length.

charging in the SEM. The gentle nature and high selectivity of the XeF_2 etch is illustrated in Figure 3, which shows 400Å thick, 2μm wide, 240μm long thermal oxide beams after 10 minutes of etching in XeF_2. These thin, fragile beams survived while 50μm of silicon were etched away from underneath. Furthermore, it was found that photoresist can be used to mask silicon etches of hundreds of microns without any apparent mask degradation.

The overall etch rate for the methods described above ranges from roughly 1μm/pulse for large exposed areas (a few cm^2) to 40μm/pulse for small areas (hundreds of μm^2). For a pulse duration of 1 minute the average etch rate is 5-10μm/pulse. Constant pressure etching produces a slightly slower silicon etch rate compared to pulse etching (3-5μm/min at 2500mTorr).

5. LOADING AND APERTURE EFFECTS

The size of the exposed silicon area can affect the etch rate. In general, the etch rate decreases as the exposed area

Downloaded From: http://proceedings.spiedigitallibrary.org/ on 10/23/2015 Terms of Use: http://spiedigitallibrary.org/ss/TermsOfUse.aspx

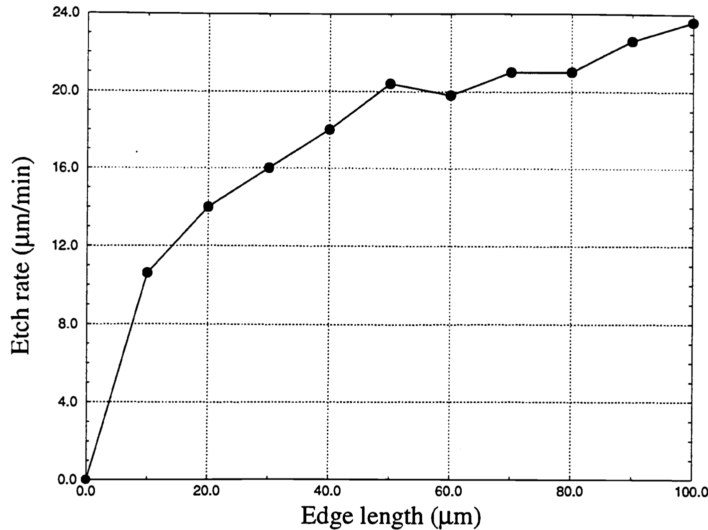

Fig. 5. Graph of etch rate vs. edge length for isolated square-shaped etch windows ranging from 10µm to 100µm on a side illustrating the aperture effect. The etch time was 5 minutes for each run.

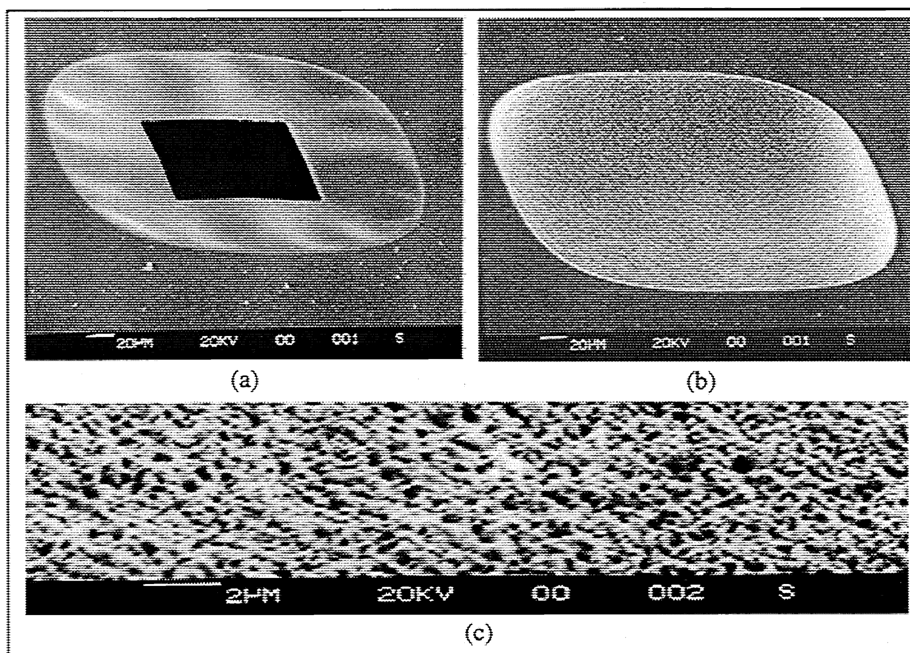

Fig. 6. SEM photographs of a silicon wafer patterned with an isolated 100µm etch window. (a) After 2 minutes of XeF_2 etching. The silicon dioxide mask is still in place. (b) After 3 minutes of XeF_2 etching. The silicon dioxide mask has been removed by an additional 49% HF etch to show the silicon pit. (c) SEM close-up in the pit showing grainy surface morphology.

increases, presumably due to the depletion of XeF_2 (loading effect). For smaller etch windows (square exposed silicon areas on the order of 10µm on a side), the etch rate increases as the exposed area (or aperture) increases, presumably due to an aperture dependent flow or diffusion resistance. To investigate the loading effect, several isolated square openings from 1mm to 10mm on a side were etched using 1 - 6 pulses of XeF_2, with each pulse lasting one minute. The resulting data is shown in Figure 4. Squares less than 4mm on a side etched at roughly 20µm/min, while squares with 8 or 10mm on a side etched less than half as fast.

Downloaded From: http://proceedings.spiedigitallibrary.org/ on 10/23/2015 Terms of Use: http://spiedigitallibrary.org/ss/TermsOfUse.aspx

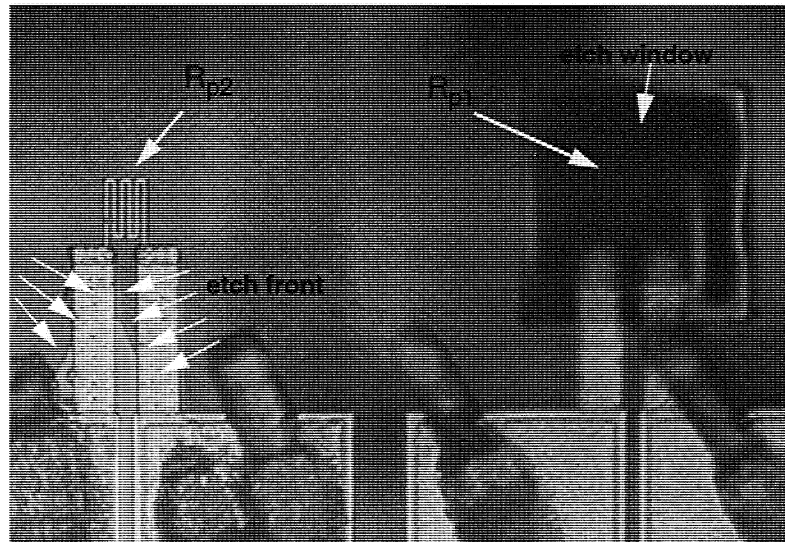

Fig. 7. Optical microscope photograph of polysilicon resistors after 47 minutes of constant pressure (2500mT) XeF_2 etching. The etch depth was 290μm, undercut was 150μm. There is residual oxide in the etch window surrounding R_{p1}. Also, R_{p1} is out of focus because residual stress in the oxide caused a 17μm deflection out of the plane of the substrate. The etch fronts from two separate etch windows are marked in the photo.

To investigate the aperture effect, several isolated square openings from 10 to 100μm on a side were etched at constant pressure (2000mT) for 5 minutes. As shown in Figure 5, the large openings etched twice as fast as the smaller openings. Figure 6a show a SEM photograph of a silicon pit etched out by XeF_2 with an etch window of 100μm on a side. The silicon dioxide mask was later removed using a hydrofluoric acid etch to expose the silicon pit underneath (Fig. 6b). These rounded pits are typical of those obtained in this experiment and exhibit a grainy surface (Fig. 6c) with a surface roughness on the order of 0.1μm.

6. THERMAL EFFECTS

Another important parameter affecting the silicon etch rate is temperature. According to the data from Flamm et al.[13], one would expect a one percent decrease in etch rate for a one degree increase in temperature above room temperature. Since the XeF_2 etch reaction is quite exothermic (generating on the order of 1 W/cm^2 of etch area for typical etch rates), the heat generated by the reaction may substantially lower the reaction rate. To investigate these effects, electrical measurements were made during etching using polysilicon and aluminum resistor test structures fabricated through the MOSIS foundry service using Orbit Semiconductor's 2μm double poly, double metal CMOS process. Since both polysilicon and aluminum exhibit an increase in resistance with an increase in temperature, the experimental results can be used to gather information about the thermal processes taking place during etching. The thermal coefficient of resistance of polysilicon was measured to be roughly $10^{-3}/^{o}C$, while that for aluminum is reported to be $3 \times 10^{-3}/^{o}C$. The thermal time constant of these CMOS chips is calculated to be roughly 0.5 seconds. The chips were bonded to 28-pin DIP packages using 5-minute epoxy. Each chip was then wire-bonded to the package, which was placed onto a prototype circuit board. A barrier block was used to make the connection to the electrical feedthroughs in the XeF_2 etching system. Data was read from two digital multimeters at 10-second intervals during the course of the etch. All chips were etched at a constant pressure of 2500mTorr, and all thin film resistors were encased in silicon dioxide.

6.1 Thermal effects on polysilicon resistors

The first experiment to investigate the thermal effect of XeF_2 etching was conducted on two identical polysilicon resistors, both of which were encapsulated in a sheet of multilayered CMOS dielectric (silicon dioxide) roughly 3μm thick. A ring of exposed silicon was patterned around the test resistor, R_{p1}, creating a 60μm x 70μm silicon dioxide plate isolated from the rest of the silicon dioxide. The exposed silicon acts as an etch window for the undercutting of structures such as the silicon

Downloaded From: http://proceedings.spiedigitallibrary.org/ on 10/23/2015 Terms of Use: http://spiedigitallibrary.org/ss/TermsOfUse.aspx

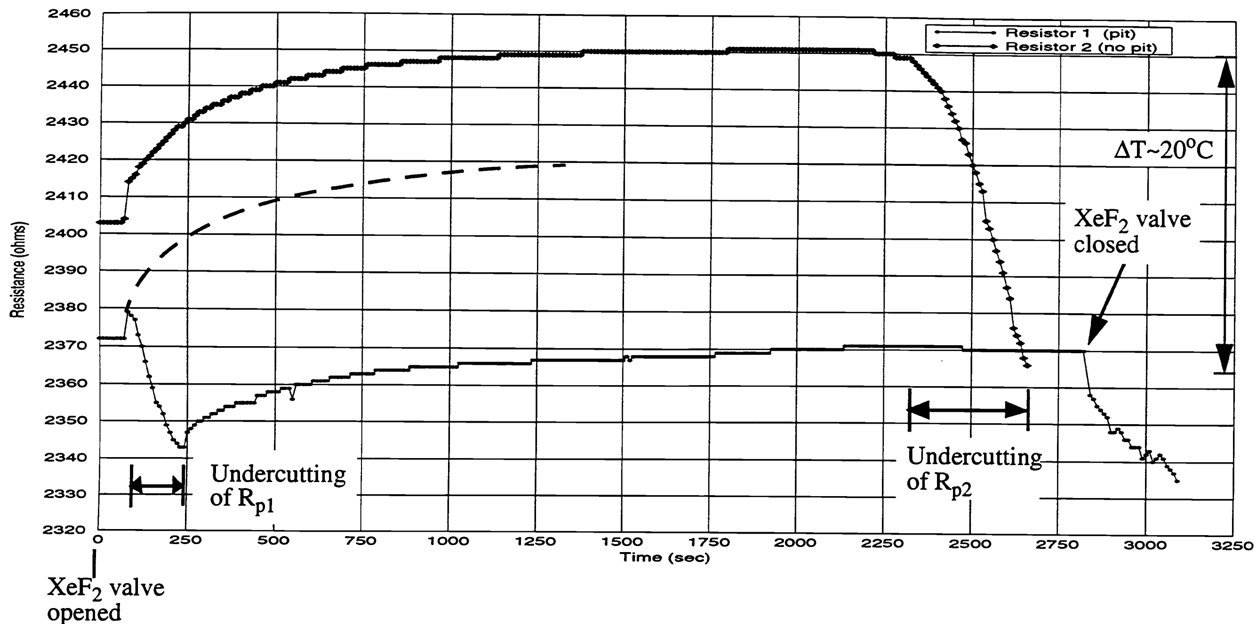

Fig. 8. Graph of change in resistance vs. time for the two polysilicon resistors shown in Fig. 7 during a 47 minute XeF_2 etch. The decrease in R_{p1} between time ~100-250 seconds is believed to be a piezoresistive effect due to relief of residual stress as the oxide/poly/oxide composite thin film is undercut. The exponential increase and decrease in R_{p2} is due to etching-induced substrate heating.

dioxide plate. Two 20μm wide aluminum beams running across part of the etch window act as both electrical connection to the resistor and cantilever support for the silicon dioxide plate after release[7]. The control resistor, R_{p2}, was located away from etch windows to prevent undercutting. Figure 7 shows R_{p1} and R_{p2} after a 47 minute etch. During the etch, the resistances of R_{p1} and R_{p2} were recorded in ten second intervals (Fig. 8).

For polysilicon resistors, we expect to observe both thermal and piezoresistive effects. The thermal effect is described first. During the course of the etch, both resistors exhibited periods of rising resistance. The resistance of R_{p2} rose between the times of 80 to 2250 seconds and the resistance of R_{p1} rose between the times of 80 to 2800 seconds, except for a drop just before 250 seconds. These increases in resistance are presumably due to substrate heating from the exothermic etch. At 2480 seconds, the XeF_2 inlet valve was closed and the resistance of R_{p1} dropped abruptly, presumably due to the substrate cooling. The reason for the 80 second delay before the expected changes in resistance is as yet unclear.

In addition to the observed thermal effects, we believe the resistors also exhibited piezoresistive effects. Resistor R_{p1} generally rose in resistance during etching except from ~100 to 250 seconds, when the resistance momentarily dropped. This drop corresponds to the undercutting of the silicon dioxide plate that encased R_{p1}. When silicon dioxide is undercut, it relieves its residual stress by expansion. The expansion strains the encapsulated resistor, causing the resistance to change. Since it took roughly 150 seconds to undercut a 60μm x 70μm plate, the lateral etch rate was approximately 18μm/min. As R_{p1} was undercut, the etch front from the etch window progressed toward R_{p2}. At an equal distance on the other side of R_{p2} was a similar etch window. Since the two etch windows were roughly the same distance from R_{p2}, the etch fronts were expected to intersect beneath R_{p2} as shown in Figure 7. At 2250 seconds, resistor R_{p2} showed a similar drop in resistance as that of R_{p1}, which indicated undercutting of R_{p2}. The drop in resistance abruptly ended at 2670 seconds when R_{p2} became an open circuit. Subsequent examination of the resistor showed a discoloration in R_{p2} that may have been caused by XeF_2 etching, though no cracks were apparent in the silicon dioxide. This was the only instance in which a polysilicon resistor was observed to have been damaged during a XeF_2 etch. Since R_{p2} was encapsulated in a contiguous sheet of silicon dioxide, it would experience more strain as it was being undercut. Figure 8 shows R_{p2} does have a higher change in resistance (~85Ω) than R_{p1} (~55Ω), indicating more strain in R_{p2}. This strain may have caused a crack under the resistor as the etch front passed underneath it, exposing the resistor to XeF_2. R_{p1}, which was encapsulated in an isolated silicon dioxide plate, would experience less strain and therefore not give the same result. Usually, we undercut smaller silicon dioxide structures that are separated from the rest of the silicon

Downloaded From: http://proceedings.spiedigitallibrary.org/ on 10/23/2015 Terms of Use: http://spiedigitallibrary.org/ss/TermsOfUse.aspx

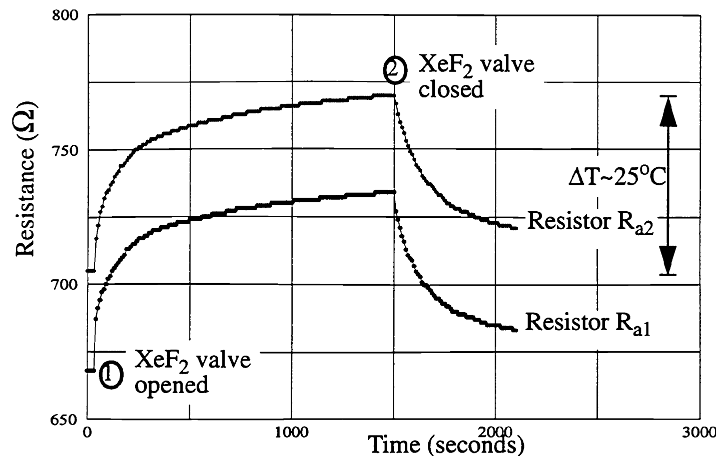

Fig. 9. Graphs of change in resistance over time for aluminum resistors encased in oxide. Initial resistance of $R_{a1} = 668\Omega$. Initial resistance of $R_{a2} = 705\Omega$. R_{a1} was partially undercut in XeF_2, while R_{a2} was fully protected.

dioxide, like R_{p1}, so the silicon dioxide expansion does not cause problems.

6.2 Thermal effects on aluminum resistors

To observe only the thermal effects, a separate experiment was conducted using aluminum resistors, instead of polysilicon resistors. Both resistors were encased in silicon dioxide and had etch windows surrounding them, but the second resistor, R_{a2}, was protected by photoresist to prevent undercutting. Both resistors were identical but were located on different chips. The difference in initial resistance is attributed to non-uniformities from chip to chip in the fabrication process. Although resistor R_{a1} was surrounded by exposed silicon, it was not completely undercut because the etch was terminated when the etch front reached the edge of the encased aluminum. The aluminum resistors were etched simultaneously for a total of 35 minutes. The data is shown in Figure 9. At time zero, the XeF_2 valve was opened, and etching of the exposed silicon areas began. 40 seconds later, the resistance increased simultaneously for R_{a1} and R_{a2} (point 1). This rise continued until 1510 seconds, when the XeF_2 valve was closed and the chamber was pumped down (point 2). Both resistors then exhibited an exponential decrease in resistance. Measurements of the resistances were taken for an additional 10 minutes after the etch had ended.

6.3 Observations from thermal experiments

From the experimental data, several observations can be made. During XeF_2 etching, all resistors exhibited an exponential resistive change with a time constant τ of approximately 250 seconds. This appears to be the thermal time constant of the package/support structure of the chip. It is unclear as to why there is a minute-long delay of the onset of resistance change. All resistors indicate a change in temperature ΔT of approximately 20-30°C. Although the aluminum resistor R_{a2} was masked by photoresist, it exhibited the same amount of change in resistance as the unmasked resistor R_{a1} during the experiment, indicating that the temperature distribution on the silicon chip surface was relatively uniform. This implies that the temperature sensed by a resistor anywhere on the chip during a XeF_2 etch is roughly the same temperature at the etch fronts. The polysilicon piezoresistors show a dramatic drop in resistance as they are undercut, possibly indicating a relief of residual compressive stress in the encapsulating silicon dioxide layers. Assuming an n-type polysilicon gauge factor of -20, the observed change in resistance corresponds to a residual strain of ~0.1%.

7. ETCH UNIFORMITY

The uniformity across a wafer etched in XeF_2 was also investigated. A silicon dioxide mask on a 3-inch silicon wafer was patterned with a 2-dimensional array of 0.5mm square openings on 1.125mm centers over a circular area 5cm in diameter, for a total exposed area of 3.4cm^2. One wafer was continuously etched at 2500 mTorr for 10 minutes, while the other was pulse etched in 10 pulses of one minute duration each. In both cases the wafer flats were aligned to the XeF_2 inlet. The resulting etch

Downloaded From: http://proceedings.spiedigitallibrary.org/ on 10/23/2015 Terms of Use: http://spiedigitallibrary.org/ss/TermsOfUse.aspx

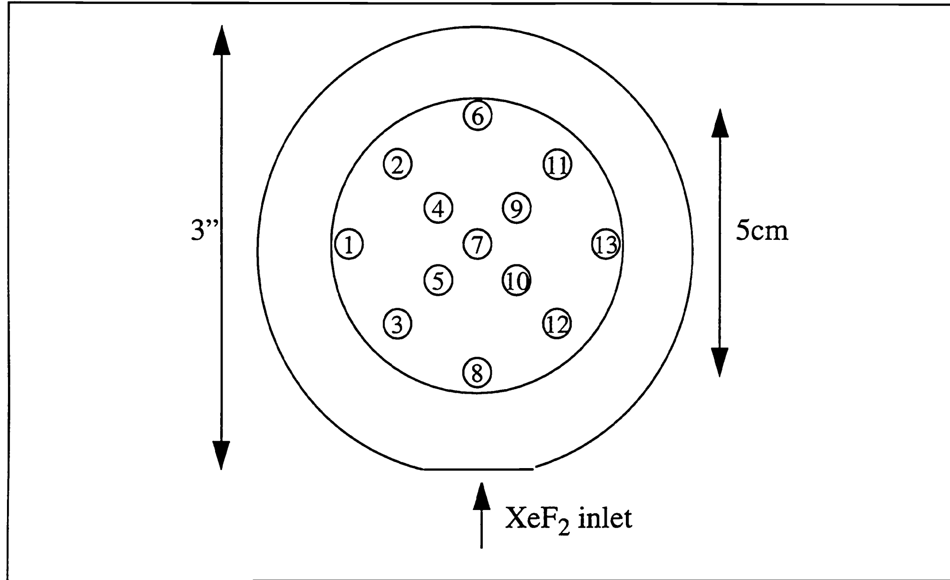

Fig. 10. Map of wafer positions at which etch depth measurements were taken.

Table 1 Etch depth for different locations on wafer

Location (refer to Figure 10)	Etch depth (μm) for constant pressure etching	Etch depth (μm) for pulse etching	Percent difference in etch depth
1	13.89	17.39	25.2
2	12.72	16.00	25.8
3	19.58	19.94	1.8
4	6.50	8.99	38.3
5	8.32	10.74	29.1
6	11.99	16.47	37.4
7	5.84	8.43	44.3
8	20.74	21.69	4.6
9	6.48	9.05	39.7
10	8.51	11.23	32.0
11	12.12	15.66	29.2
12	19.01	20.12	5.8
13	15.53	17.99	15.8

depths were measured at 13 of the 1350 locations on each wafer, as shown in Figure 10. The data is shown in Table 1.

There are several similarities in the data for the constant pressure and pulse etches. In both cases, the highest etch rates were seen on the edge of the wafer closest to the XeF_2 inlet, and the slowest etching occurred at the middle of the wafer. Etch

Downloaded From: http://proceedings.spiedigitallibrary.org/ on 10/23/2015 Terms of Use: http://spiedigitallibrary.org/ss/TermsOfUse.aspx

rates in both cases increase with distance from the center of the wafer. Although both etches display very poor uniformity, the pulse etch has slightly better uniformity overall. Etch uniformity could be substantially improved with a more uniform gas distribution system. The data indicates that pulse etching is between 2% and 44% faster than constant pressure etching, with an average increase in etch rate of 25%. In both cases the average etch rate is on the order of 1μm/min. According to Figure 4, we would expect a much higher etch rate for an isolated 0.5mm square, suggesting a loading effect due to the simultaneous etching of the array of etch windows.

8. DISCUSSION

Several techniques have been developed to improve the yield of XeF_2 etched structures. First, caution is needed to design structures that allow residual stress to be relieved without exceeding the strain limit of the structural material. Additional design rules are needed to insure that the electronics and bonding pads are far enough from etch windows to prevent unwanted undercutting. Patterning etch holes in structures designed for release helps decrease the required etch time and results in less unwanted undercutting. However, before exposure to XeF_2, etch windows in the mask must be etched clean of the masking material because of the high selectivity of XeF_2. Generally, the etch rates range from roughly 1μm/min for wafer scale etches and roughly 5μm/min for commercial chip etches. Etch uniformity is poor for full wafer etches but could be improved by modifications to the XeF_2 gas distribution system. Lastly, samples must be carefully dehydrated to allow etching of silicon to occur.

XeF_2 is a silicon etchant that offers many advantages over traditional etchants such as EDP and KOH. Since XeF_2 has a high selectivity to aluminum, photoresist, and silicon dioxide, and etching is conducted in gas-phase at room temperature, integrating bulk micromachined structures with standard CMOS electronics can be achieved without significant changes to the fabrication process. Oxide structures with polysilicon piezoresistors can be patterned during CMOS fabrication and released from the silicon substrate by a post-process XeF_2 etch step. CMOS electronics, including amplifiers, showed no signs of operational degradation after exposure to XeF_2. In addition, since XeF_2 has a high selectivity to aluminum and polymers, novel bulk micromachined structures can be created from these materials. Furthermore, XeF_2 does not have the adhesion and stiction problems associated with liquid-phase etchants so fragile, compliant structures can be fabricated. These properties make XeF_2 a useful addition to the conventional bulk silicon etchants. The lack of etch stop and crystal plane selectivity limits the utility for traditional bulk operations such as making membranes, proof masses, and p+ piezoresistors.

9. ACKNOWLEDGMENTS

Many thanks to Dr. Eli Yablonovitch for seminal discussions on selective silicon etching, and to Puthear Som, Beverley Eyre, Makoto Miura, and Misti Christianson for their help. This work was supported in part by the National Science Foundation (NSF) under grant ECS-9311975 and by NSF and ARPA under grant IRI-9321718.

10. REFERENCES

1. K. Petersen, "Silicon as a mechanical material," *Proceedings of the IEEE*, Vol. 70, No. 5, pp. 420-457, May 1982.
2. O. Tabata, "pH-Controlled TMAH etchants for silicon micromachining," *The 8th International Conference on Solid State Sensors and Actuators (Transducers '95)*, Vol. 1, pp. 83-85, 1995.
3. N. Bartlett, "Xenon hexafluoroplatinate(v) $Xe^+[PtF_6]^-$," *Proceedings of the Chemical Society*, p. 218, London, June 1962.
4. C.L. Chernick, H.H. Claassen, P.R. Fields, H.H. Hyman, J.F. Malm, W.M. Manning, M.S. Matheson, L.A. Quarterman, F. Schreiner, H.H. Selig, I. Sheft, S. Siegel, E.N. Sloth, L. Stein, M.H. Studier, J.L. Weeks, M.H. Zirin, "Fluorine Compounds of Xenon and Radon," Science, Vol. 138, pp. 136-138, October 1962.
5. H. F. Winters and J. W. Coburn, "The etching of silicon with XeF_2 vapor," *Applied Physics Letters,* Vol. 34, No. 1, pp. 70-73, January 1979.
6. F. A. Houle, "A reinvestigation of the etch products of silicon and XeF_2: doping and pressure effects," *Journal of Applied Physics*, Vol. 60, No. 9, pp. 3018-3027, 1986.
7. D. L. Flamm, D. E. Ibbotson, J. A. Mucha, and V. M. Donnelly, "XeF_2 and F-atom reactions with Si: their significance for plasma etching," *Solid State Technology,* pp. 117-121, April 1983.
8. E. Hoffman, B. Warneke, E. J. J. Kruglick, J. Weigold, and K.S.J. Pister, "3D structures with piezoresistive sensors in standard CMOS," *Proceedings of Micro Electro Mechanical Systems Workshop (MEMS '95)*, pp. 288-293, 1995.
9. B. Eyre, K. S. J. Pister, and W. Gekelman, "Multi-axis micro-coil sensors in standard CMOS," *Proceedings of the SPIE*

Downloaded From: http://proceedings.spiedigitallibrary.org/ on 10/23/2015 Terms of Use: http://spiedigitallibrary.org/ss/TermsOfUse.aspx

1995 Symposium on Micromachining and Microfabrication, Austin, Texas, October 23 - 24 1995 (in press).

10. B. Warneke, E. Hoffman, K. S. J. Pister, "Monolithic multiple axis accelerometer design in standard CMOS," *Proceedings of the SPIE 1995 Symposium on Micromachining and Microfabrication*, Austin, Texas, October 23 - 24 1995 (in press).
11. E. J. J. Kruglick, S. Damle, K. S. J. Pister, "Three-dimensional structures for micro-optical mechanical systems in standard CMOS," *Proceedings of the SPIE 1995 Symposium on Micromachining and Microfabrication*, Austin, Texas, October 23 - 24 1995 (in press).
12. J. W. Coburn and H. F. Winters, "Ion- and electron-assisted gas-surface chemistry -- an important effect in plasma etching," *Journal of Applied Physics*, Vol. 50, No. 5, pp. 3189-3196, May 1979.
13. D. L. Flamm and V. M. Donnelly, "The design of plasma etchants," *Plasma Chemistry and Plasma Processing*, Vol. 1, No. 4, pp. 317- 363, 1981.
14. Aldrich Chemical Company, Inc., 2905 West Hope Avenue, Milwaukee, WI 53216.
15. Alpha Aesar, 30 Bond Street, Ward Hill, MA 01835.
16. PCR Inc., P.O. Box 1466, Gainesville, FL 32602.
17. Neil Bartlett, personal communication.

Downloaded From: http://proceedings.spiedigitallibrary.org/ on 10/23/2015 Terms of Use: http://spiedigitallibrary.org/ss/TermsOfUse.aspx